Cyclophilin D is a component of mitochondrial permeability transition and mediates neuronal cell death after focal cerebral ischemia

Anna C. Schinzel*†, Osamu Takeuchi*‡, Zhihong Huang§, Jill K. Fisher*, Zhipeng Zhou§, Jeffery Rubens*, Claudio Hetz*, Nika N. Danial*, Michael A. Moskowitz†§, and Stanley J. Korsmeyer*

*Howard Hughes Medical Institute and Dana–Farber Cancer Institute, Harvard Medical School, 44 Binney Street, Boston, MA 02115; ‡Department of Host Defense, Research Institute for Microbial Diseases, Osaka University, Suita, Osaka 565-0871, Japan; and §Stroke and Neurovascular Regulation Laboratory, Massachusetts General Hospital, Harvard Medical School, 149 13th Street, Charlestown, MA 02129

Communicated by Bruce M. Spiegelman, Harvard Medical School, Boston, MA, June 23, 2005 (received for review May 31, 2005)

Mitochondrial permeability transition (PT) is a phenomenon induced by high levels of matrix calcium and is characterized by the opening of the PT pore (PTP). Activation of the PTP results in loss of mitochondrial membrane potential, expansion of the matrix, and rupture of the mitochondrial outer membrane. Consequently, PT has been implicated in both apoptotic and necrotic cell death. Cyclophilin D (CypD) appears to be a critical component of the PTP. To investigate the role of CypD in cell death, we created a CypD-deficient mouse. *In vitro*, CypD-deficient mitochondria showed an increased capacity to retain calcium and were no longer susceptible to PT induced by the addition of calcium. CypD-deficient primary mouse embryonic fibroblasts (MEFs) were as susceptible to classical apoptotic stimuli as the WT, suggesting that CypD is not a central component of cell death in response to these specific death stimuli. However, CypD-deficient MEFs were significantly less susceptible than their WT counterparts to cell death induced by hydrogen peroxide, implicating CypD in oxidative stress-induced cell death. Importantly, CypD-deficient mice displayed a dramatic reduction in brain infarct size after acute middle cerebral artery occlusion and reperfusion, strongly supporting an essential role for CypD in an ischemic injury model in which calcium overload and oxidative stress have been implicated.

mitochondria | oxidative stress | calcium homeostasis

Numerous toxic stimuli convert mitochondria from a life-sustaining organelle to an inducer of cell death (1–3). In response to cell death stimuli, prodeath proteins sequestered in the inner mitochondrial membrane space are released into the cytosol upon disruption of the mitochondrial outer membrane (MOM) (4–6). The proapoptotic BCL-2 family members BAX and BAK constitute a "gateway" to the apoptotic program by regulating events leading to disruption of the MOM (7). BCL-2 family members not only function at the MOM but also are located at the endoplasmic reticulum (ER), where they regulate calcium fluxes. By controlling steady-state calcium levels in the ER, BCL-2 family members regulate the amount of calcium released from the ER to transmit a death signal mediated by mitochondrial calcium uptake (8–11).

Sequestration of high levels of calcium by mitochondria can also lead to disruption of the MOM, which, mechanistically, is thought to occur by means of the phenomenon of permeability transition (PT). PT is described as an abrupt increase of inner membrane permeability to solutes with molecular masses of <1,500 Da. These events are caused by the opening of a highly regulated channel [PT pore (PTP)], which leads to dissipation of the mitochondrial transmembrane potential and an influx of solutes, causing expansion of the matrix (reviewed in ref. 12). The latter event may result in sufficient swelling to rupture the MOM and cause cytochrome *c* release and subsequent caspase activation, resulting in apoptosis. However, dissipation of the membrane potential can also lead to a sudden decrease in ATP levels. Although caspase-dependent apoptosis requires ATP, a sudden decrease in ATP levels can alternatively induce necrotic cell death (13, 37).

Currently, two models describe the molecular organization of the PTP. In the first model, the PTP is formed at contact sites between the inner and outer mitochondrial membranes and consists of the voltage-dependent anion channel, the adenine nucleotide translocator (ANT), and cyclophilin D (CypD), the mitochondrial isoform of the peptidylprolyl *cis-trans* isomerase cyclophilin chaperone family (14–16). ANT acts as a regulatory component of the PTP, although it doesn't seem to be essential and may be redundant (17, 18). A second model suggests that CypD and chaperone-like proteins suppress the misfolding and aggregation of native membrane proteins. In this formulation, an increase in matrix calcium opens the PTP by perturbing the interaction between CypD and aggregated proteins (19).

Although the structural components of the PTP remain undefined, the physiological role of PT *in vitro* and *in vivo* has been extensively described. *In vitro* PT is induced by the mitochondrial sequestration of high levels of calcium and is regulated by factors such as low ATP levels and oxidative stress (20, 37). These conditions, which are required for the activation of PT, develop in neuronal cell cultures subjected to oxidative stress, excitotoxicity, and oxygen-glucose deprivation. In these settings, the sequestration of high levels of calcium by mitochondria is suggested to be the underlying cause of cell death (21, 22). *In vivo* parameters required for the induction of PT are mimicked during ischemia/reperfusion in the brain. During brain ischemia, the absence of glucose and oxygen causes mitochondrial dysfunction, intracellular calcium uptake, and a decrease in ATP levels. Brain reperfusion generates conditions required for PT as mitochondria repolarize, sequester excess cytosolic calcium acquired by cells during the ischemic period, and subsequently generate oxidative stress (reviewed in refs. 23 and 24). Cells die by both necrotic and apoptotic cell death during ischemia/reperfusion. Necrosis is thought to occur in the ischemic territory (core), characterized by extreme hypoperfusion, whereas apoptotic-like cell death is unmasked in the surrounding penumbra (reviewed in refs. 25 and 26).

Although PT is clearly implicated in many types of cell death, the essential components of the PTP remain uncertain. CypD is targeted by the immunosuppressant drug cyclosporin A (CsA),

Abbreviations: CypD, cyclophilin D; PT, permeability transition; PTP, PT pore; ER, endoplasmic reticulum; ANT, adenine nucleotide translocator; MOM, mitochondrial outer membrane; MEF, mouse embryonic fibroblast; MCAo, middle cerebral artery occlusion; CsA, cyclosporin A; EB, experimental buffer; KO, knockout.

†To whom correspondence may be addressed. E-mail: anna_schinzel@dfci.harvard.edu or michael_moskowitz@mgh.harvard.edu.

BIOCHEMISTRY

which interacts with CypD and inhibits the opening of the PTP (27). In isolated mitochondria, the addition of CsA inhibits mitochondrial swelling and increases mitochondrial calcium retention capacity (28). An investigation of the role of PT in cultured cells has relied on CsA and CypD overexpression studies, which have described its function in both apoptosis and necrosis (29–31). *In vivo*, the inhibitory effect of CsA emphasized the critical importance of PT in cell death induced by ischemia/reperfusion. In models of ischemic brain injury, treatment with CsA or its analogue, *N*-methyl-valine-4 CsA, significantly decreases infarct size (32–34). However, the importance of CypD *in vivo* and in cell culture remains poorly understood because of the pleiotropic nature of CsA.

Here, we show that CypD is an essential component of PT *in vitro* and *in vivo*. Cell death assays show that CypD does not appear to play a role in cell death in response to multiple apoptosis-inducing stimuli but plays a central role in cell death induced by H_2O_2 (hydrogen peroxide), a generator of oxidative stress. Furthermore, CypD deficiency confers significant protection against ischemic brain injury in a middle cerebral artery occlusion (MCAo) model, suggesting an *in vivo* role in cell death. These data suggest that CypD may be an important determinant of cell and tissue death and provide a selective therapeutic target.

Materials and Methods

Animal Handling and Treatment. All mice were handled according to Dana–Farber Cancer Institute, Massachusetts General Hospital, and Harvard Medical School institutional guidelines on animal care.

Generation of CypD-Deficient Mice. The *CypD* gene was isolated from genomic DNA extracted from RW4 ES cells by PCR. A targeting vector was constructed to flank exons 3–5 with two *loxP* sites. The *loxP* site-flanked *Neo*^{r} gene fragment was inserted into the intron of the *CypD* gene. A 1-kb 5′ upstream genomic fragment and 3′ downstream 6-kb genomic fragment were inserted. The linearized vector was electroporated into RW4 ES cells. After selection with G418, drug-resistant clones were picked and screened by PCR and Southern blot analysis. The homologously recombined clones were transiently transfected with a pMC-Cre gene to delete the neo gene. Clones that showed G418 sensitivity were subjected to Southern blot analysis to detect the floxed *CypD* and null alleles. These clones were individually microinjected into blastocysts derived from C57BL/6 mice to obtain chimeric mice. The targeted alleles were successfully transmitted through the germ line.

Preparation of Mitochondria. Mitochondria were isolated from the livers of mice by standard differential centrifugation and resuspended in isolation buffer (0.2 M sucrose/10 mM Tris-Mops, pH 7.4/0.1 mM EGTA-Tris) and stored on ice. Mitochondria were used immediately after preparation. Mitochondrial protein content was quantified by using the BCA protein assay (Pierce).

Mitochondrial Swelling. Mitochondria (0.5 mg/ml) were incubated in experimental buffer (EB) (125 mM KCl/10 mM Tris-Mops, pH 7.4/1 mM Pi/5 mM glutamate/2.5 mM malate/10 μM EGTA-Tris, pH 7.4) for 5 min in the presence or absence of 1 μM CsA before experiments were started. The swelling of mitochondria caused by an influx of solutes across the inner membrane was measured by recording the decrease in absorbance at 540 nm on a Beckman DU 640 spectrophotometer.

Calcium Buffering Capacity of the Mitochondria. Mitochondrial uptake of calcium was determined fluorometrically by using the calcium indicator Calcium Green 5N (Molecular Probes). Mitochondria (0.5 mg/ml) were added to a well stirred quartz cuvette at 24°C containing 0.5 ml of EB and 1 μM Calcium Green 5N. The cuvette was placed in a spectrophotometer, and extramitochondrial calcium was monitored by following the fluorescence with an excitation of 506 ± 2.5 nm and an emission of 531 ± 5.0 nm.

Electron Microscopy. Mitochondria were fixed for 1 h at 25°C by using gluteraldehyde dissolved in EB at a final concentration of 1.25%, embedded in plastic, sectioned, and stained with uranyl acetate and lead citrate. Thin sections were imaged on a JEOL 1200EX transmission electron microscope.

Cell Culture and Induction of Apoptosis. Mouse embryonic fibroblast (MEF) cultures were established from embryonic day-13.5 embryos according to standard procedures. MEFs were maintained in DMEM plus 10% FCS, L-glutamine, and penicillin/streptomycin (Invitrogen). For apoptosis induction, MEFs were plated in 12-well plates and grown for 24 h before treatment. Apoptosis was detected by flow cytometric detection of annexin V and propidium iodide staining after the induction of cell death.

Transient Focal Cerebral Ischemia by Acute MCAo. CypD-deficient mice and WT mice from the same litter (littermates) were used for all experiments. Only male mice matched for age (6–12 weeks) were used for experiments. Cerebral ischemia was induced by an intraluminal filament as described in ref. 35 by an investigator who was naïve to the genetic identity of individual mice.

Results

Generation of CypD-Deficient Mice. To assess the role of CypD *in vivo*, we generated a conditional CypD null mutant by generating a targeting vector in which *loxP* sites flank exons 3, 4, and 5 of the murine CypD (Fig. 1*A*). This CypD^{flox} allele was transmitted through the germ line. The floxed allele was crossed to the EIIa transgenic cre line to generate a null allele. Breeding of CypD$^{WT/null}$ mice yielded viable CypD$^{null/null}$ mice at the expected Mendelian frequency. The CypD$^{null/null}$ mice appeared to have no gross abnormal phenotype, including a normal appearing brain and cerebrovasculature. PCR was used to detect and confirm the presence of the knockout (KO) and WT alleles (Fig. 1*B*). Successful deletion of CypD in mitochondria purified from the liver of CypD$^{null/null}$ mice was confirmed by immunoblotting using an antibody directed against a peptide sequence encoded in exon 1 of the *CypD* gene (Fig. 1*C*).

CypD Is Essential for Calcium-Induced PT *in Vitro*. To investigate the importance of CypD for the PT, mitochondria were isolated from the liver of CypD$^{WT/WT}$ and CypD$^{null/null}$ mice. CypD$^{WT/WT}$ and CypD$^{null/null}$ mitochondria were able to take up the cationic dye rhodamine 123 (data not shown), indicating the presence of a functional transmembrane potential. Opening of the PTP was followed by an increase of inner membrane permeability to solutes with a molecular mass of <1,500 Da, resulting in an increase in mitochondrial volume (swelling), which was monitored at an absorbance of 540 nm. CypD$^{WT/WT}$ and CypD$^{null/null}$ mitochondria were treated with 100 μM $CaCl_2$ and monitored for 10 min. CypD$^{WT/WT}$ mitochondria underwent swelling within 100 s, which was inhibitable by CsA, a pharmacological inhibitor of the PTP (Fig. 2*A Left*). This observation confirmed in our system that mitochondrial swelling resulted from calcium-induced opening of the PTP. By contrast, CypD$^{null/null}$ mitochondria failed to swell under identical conditions, suggesting an essential role for CypD in induction of PT (Fig. 2*A Right*). To examine Ca^{2+}-induced

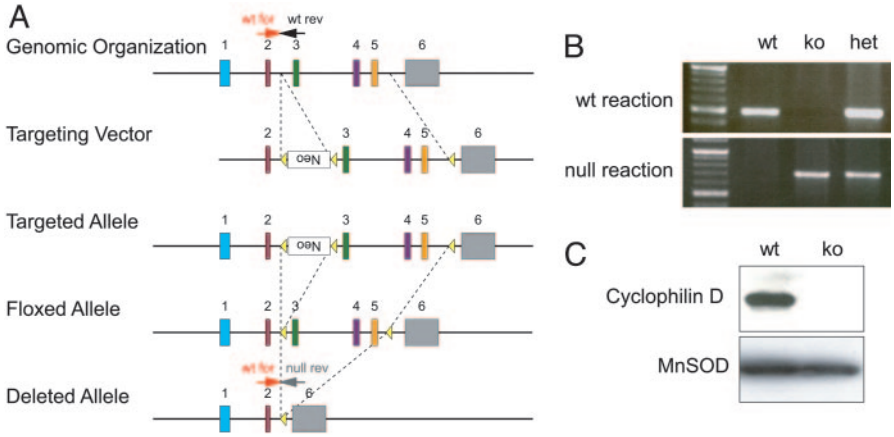

Fig. 1. Deletion of CypD. (*A*) Schematic of the CypD locus. PCR primers distinguishing WT and null alleles are designated. wt for, WT forward; wt rev, WT reverse; null rev, null reverse. (*B*) Genotyping of $CypD^{WT/WT}$ using WT forward and WT reverse primers generated a 490-bp product in the WT allele. Genotyping of $CypD^{null/null}$ mice using the null primer set WT forward and null reverse generated a 700-bp product. (*C*) Western blots of mitochondria purified from $CypD^{WT/WT}$ and $CypD^{null/null}$ mice using a CypD-specific antibody.

changes in mitochondrial morphology, mitochondria isolated from $CypD^{WT/WT}$ and $CypD^{null/null}$ livers were subjected to treatment with 100 μM $CaCl_2$ for 200 s and fixed (Fig. 2*B*). Electron microscopic analysis revealed that $CypD^{WT/WT}$ mitochondria treated with calcium displayed ruptured outer and inner membranes, matrix swelling, and disrupted cristae, which were prevented by preincubation with CsA. This observation was in striking contrast to $CypD^{null/null}$ mitochondria, which remained morphologically intact.

Next, we examined calcium homeostasis in WT and mutant mitochondria as an additional parameter of the PT. Mitochondria sequester calcium by means of the uniporter, which is critical for cellular calcium buffering (36). The ability of mitochondria to take up calcium can be assessed by measuring the disappearance of extramitochondrial free Ca^{2+} from the medium after the addition of $CaCl_2$ pulses. $CypD^{WT/WT}$ mitochondria buffered 20 μM $CaCl_2$, and their buffering capacity was significantly increased after preincubation with 1 μM CsA, consistent with the importance of the PTP in this process. $CypD^{null/null}$ mitochondria took up and buffered up to 90 μM $CaCl_2$, similar quantities of $CaCl_2$ as observed in $CypD^{WT/WT}$ mitochondria pretreated with CsA (Fig. 2*C*). Both the reduced susceptibility to Ca^{2+}-induced swelling and augmented Ca^{2+} buffering capacities in mutant mitochondria suggest that CypD is an essential component of the PT and that its ablation causes functional impairment of the PTP.

The Role of CypD in Cell Death. The role of the PTP in apoptotic and necrotic cell death has previously been defined by using the inhibitory activity of CsA (37). CsA, however, is a pleiotropic drug that affects multiple pathways. Alternatively, overexpression studies have suggested a role for CypD in both apoptosis and necrosis (29–31). To directly investigate the *in vivo* role of CypD in apoptotic cell death, we used CypD-deficient MEFs. MEFs were challenged with a multitude of death-inducing stimuli, including those that stimulate the "intrinsic" (mitochondrial-dependent) and "extrinsic" (receptor-driven) pathways of apoptosis as well as oxidative stress.

Etoposide (topoisomerase II inhibitor) and staurosporine (broad-spectrum kinase inhibitor) predominantly trigger the intrinsic, mitochondrial pathway of caspase activation. WT and CypD-deficient MEFs were equally sensitive to treatment with these agents, suggesting that the mitochondrial pathway of apoptosis can proceed independently of CypD (Fig. 3*A*). To examine whether CypD is a key player in cell death induced by stress signaling from the ER, CypD-deficient and WT MEFs were treated with thapsigargin (which inhibits the Ca^{2+} adenosine triphosphatase pump), tunicamycin (which inhibits N-linked glycosylation), or brefeldin A (which inhibits ER-Golgi transport). These stresses induce an irreversible loss of ER homeostasis by the accumulation of misfolded proteins that initiate an ER stress response. WT and CypD-deficient MEFs displayed no significant difference in susceptibility to treatment with these stimuli, suggesting that stress signaling from the ER does not depend on CypD to promote apoptosis (Fig. 3*B*). TNF-α and TNF-related apoptosis-inducing ligand (TRAIL) are prototypic activators of the extrinsic pathway of caspase activation mediated by death receptors (38). Depending on the cellular context, both can directly trigger apoptosis, or they activate caspases by a BID-dependent mitochondrial amplification step (39, 40). CypD-deficient and WT MEFs were equally susceptible to TNF-α and TRAIL-induced apoptosis, thus ruling out an essential role for CypD in apoptosis triggered by death receptor signaling (Fig. 3*C*).

Oxidative stress mediated by H_2O_2 causes the release of calcium from intracellular stores, which has previously been reported to induce PT-dependent cell death (9). To investigate whether CypD plays a central role in this cell death pathway, WT and CypD-deficient MEFs were treated with H_2O_2 at various concentrations and multiple time points (Fig. 3*D* and data not shown). The CypD-deficient MEFs were significantly less susceptible to cell death induced by H_2O_2, implicating CypD in this specific paradigm of cell death.

Neuroprotection in CypD-Deficient Mice. Treatment with CsA decreases infarct size after cerebral ischemia/reperfusion injury (32–34). Furthermore, conditions known to favor activation of the PTP, such as mitochondrial sequestration of calcium, generation of oxidative stress, and depletion of ATP levels, are present during ischemia/reperfusion. To determine the impact of CypD on brain injury, we used a MCAo model of ischemia/reperfusion. CypD-deficient mice and their WT littermate controls were subjected to 2 h of MCAo followed by 24 h of reperfusion. Blood flow distal to the occlusion dropped to $<20\%$ in the three groups and returned to preocclusion levels to the same extent after filament withdrawal. Physiological parameters such as the mean arterial blood pressure and partial pressure of arterial oxygen and carbon dioxide ($PaCO_2$ and PaO_2) did not differ between WT and CypD-deficient mice. Infarct size was measured by staining with triphenyl-

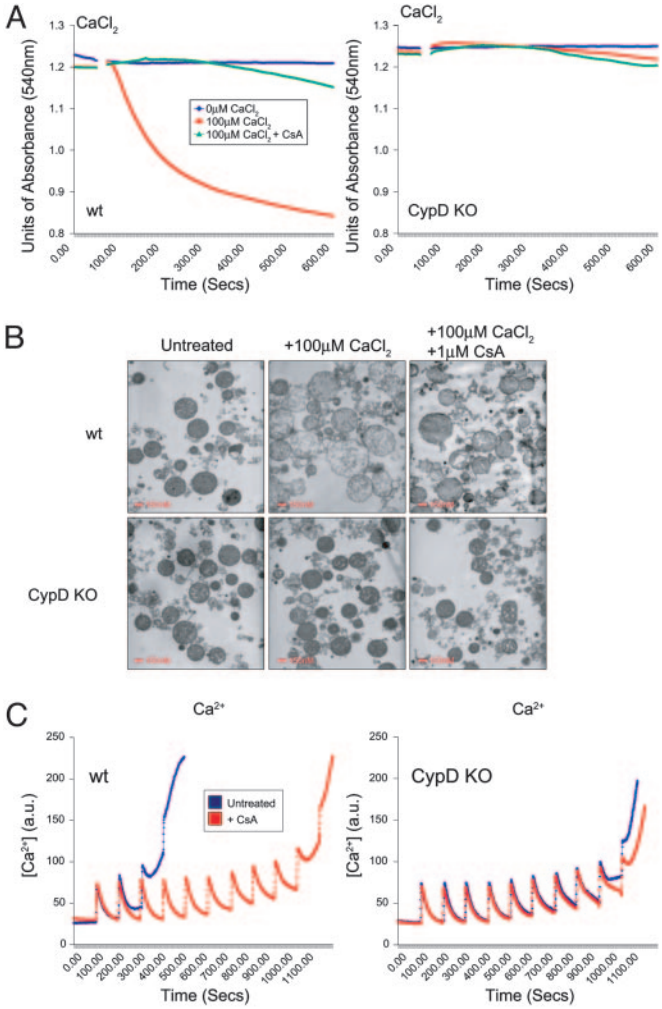

Fig. 2. Induction of PT in CypD-deficient and WT mitochondria. (*A*) Mitochondrial swelling induced by treatment with 100 μM $CaCl_2$ was measured by monitoring mitochondrial size at an absorbance of 540 nm. Mitochondria isolated from WT (*Left*) and CypD-deficient (*Right*) mice were resuspended at a concentration of 0.5 mg/ml in EB for 5 min. Where indicated (arrow), 100 μM $CaCl_2$ was added. Mitochondria were preincubated with 1 μM CsA or buffer alone for 5 min. (*B*) Transmission electron microscopy of liver mitochondria taken from WT and CypD-deficient mitochondria. Mitochondria were treated with 100 μM $CaCl_2$ for 200 s and fixed in 1.25% gluteraldehyde. (Scale bars, 200 nm.) (*C*) Loss of $CaCl_2$ buffering capacity in liver mitochondria isolated from WT and CypD-deficient mice resuspended at 0.5 mg/ml in EB. Extramitochondrial Ca^{2+} was measured fluorometrically with the calcium indicator Calcium Green 5N. Pulses of 10 μM $CaCl_2$ were added at intervals of 100 s.

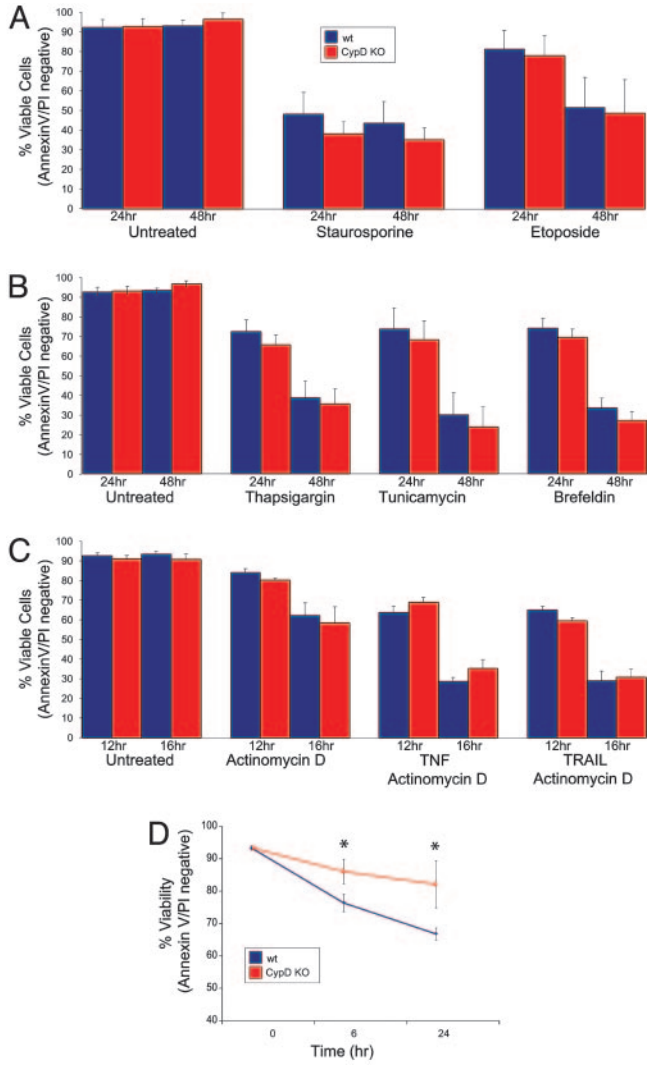

Fig. 3. Susceptibility of WT and CypD-deficient MEFs to apoptotic stimuli. (*A*) Susceptibility of MEFs to apoptotic death by mitochondria-dependent intrinsic signals. WT and CypD KO MEFs were treated with 1 μM staurosporine or 100 μM etoposide for 24 and 48 h. (*B*) Susceptibility to apoptotic cell death induced by ER stresses. WT and CypD KO MEFs were treated with thapsigargin (2 μM), tunicamycin (5 μg/μl), or brefeldin A (2 μM) for 24 and 48 h. (*C*) Susceptibility to apoptotic death by mitochondria-independent extrinsic stimuli. WT and CypD KO MEFs were treated with TNFα (1 ng/ml) or TNF-related apoptosis-inducing ligand (TRAIL) (1 μg/μl) in the presence of actinomycin D (2 μg/μl) for 12 and 16 h. (*D*) Susceptibility of WT and CypD-deficient MEFs to cell death induced by H_2O_2 (1 mM) for 16 and 20 h (*, $P < 0.05$). All error bars show SD.

tetrazolium chloride (TTC), a dye that is oxidized by intact mitochondrial dehydrogenase and yields the red product formazan. In the infarcted area, mitochondria are uncoupled and dysfunctional and no longer stain with TTC. The TTC staining characteristics of WT and mutant mice were indistinguishable in untreated brains. The infarct volume was reduced by 37% in heterozygous mice and 62% in homozygous CypD KO mice compared with their WT littermate controls (Fig. 4*A*). The area of infarct was also significantly reduced in coronal sections derived from CypD heterozygous and homozygous mice when compared with littermate controls, emphasizing the importance of CypD in ischemia/reperfusion in multiple brain regions (Fig. 4 *B* and *C*). These findings strongly suggest that CypD is a critical component of mechanisms leading to cell death during brain ischemia/reperfusion.

Discussion

In this study, we have analyzed mice with a deficiency of CypD to define its role in cell death. Our *in vitro* data show that mitochondria isolated from CypD-deficient mice have an increased capacity to retain calcium. *In vivo*, oxidative stress, such as that caused by hydrogen peroxide, induces the release of calcium from intracellular stores that is subsequently taken up by mitochondria. CypD deficiency significantly decreases the susceptibility of MEFs to hydrogen peroxide, confirming data that implicate PT in this specific paradigm of cell death (9). Conditions including oxidative stress and excessive mitochondrial calcium uptake occur during ischemia/reperfusion. In our model of MCAo-induced ischemia/reperfusion, a dramatic decrease in infarct size in the brains of CypD-deficient

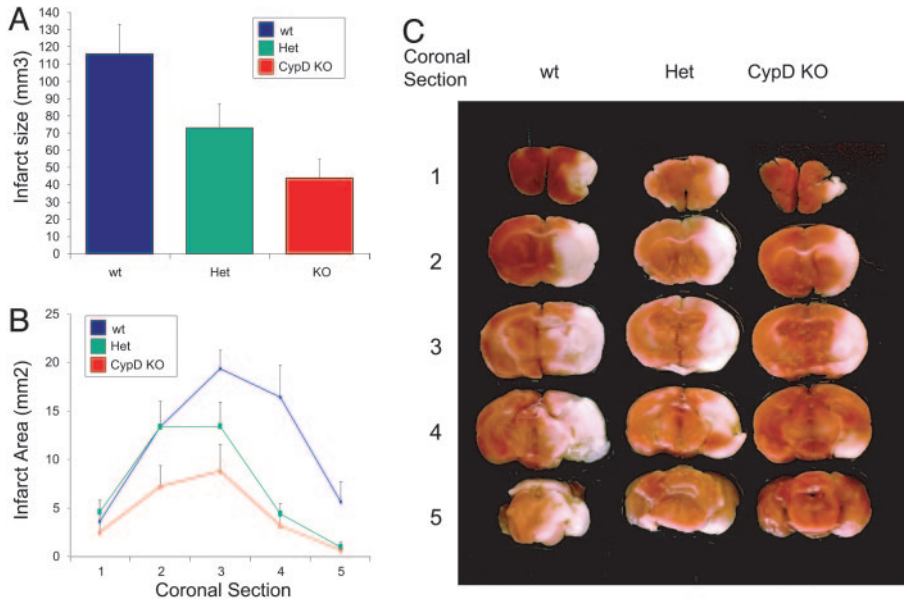

Fig. 4. Ischemia/reperfusion-mediated cell death in WT and CypD-deficient mice. (*A*) Infarct volume was reduced significantly (by 37%) in heterozygous (Het) mice and reduced by 62% in CypD KO mice compared with WT mice ($n = 9$ per group; $P < 0.05$) after 2 h of MCAo and 24 h of reperfusion. All error bars show SEM. (*B*) Protection in CypD KO mice (coronal sections 3, 4, and 5; $P < 0.05$) and heterozygous mice (coronal sections 4 and 5; $P < 0.05$) was significant in comparison with WT controls with a trend of infarct size difference at other brain section levels. (*C*) Ischemic tissue damage in CypD KO and WT mice. As shown by representative triphenyltetrazolium chloride-stained coronal brain sections, CypD KO mice had significantly smaller infarcts after 2 h of MCAo and 24 h of reperfusion (*A*) compared with WT mice.

mice suggests an essential role for CypD in cell death processes in the brain. Interestingly, heterozygous mice displayed a partial protection, demonstrating a correlation between gene dosage and the extent of injury. While the manuscript was in preparation, data published by Basso *et al.* (41), Nakagawa *et al.* (42), and Baines *et al.* (43) described a role for CypD as a target of CsA and a component of calcium-induced PT. Furthermore, Nakagawa *et al.* (42) and Baines *et al.* (43) showed that CypD plays a role in cell death in a model of cardiac ischemia/reperfusion that mimics myocardial infarction. The cardiac ischemia/reperfusion model in these studies and the paradigm presented here show that CypD is a central component of cell death pathways induced by conditions generated during ischemia/reperfusion. Collectively, our findings and these data strongly underscore the role for CypD in PT *in vitro* and in specific paradigms of cell death.

A role for CypD in PT was initially described *in vitro* by using its pharmacological inhibitor, CsA (27). Here, we show that CypD is an important component of PT and the target of CsA in isolated mitochondria, in agreement with results recently published by Basso *et al.* (41), Nakagawa *et al.* (42), and Baines *et al.* (43). CypD-deficient mitochondria are as resistant to PT-induced swelling as WT mitochondria pretreated with CsA and do not undergo the same morphological changes as WT mitochondria after induction of PT. Furthermore, CypD-deficient mitochondria buffered calcium to a similar extent as WT mitochondria pretreated with CsA, confirming the role of CypD as a key component of PT *in vitro*. Additionally, Baines *et al.* (43) generated a gain-of-function CypD model that further implicates CypD in PT. These findings strongly suggest that CypD is essential for PT-mediated swelling and are consistent with an inhibitory role for CsA on CypD in mediating changes in mitochondrial ultrastructure (5). CypD has been shown to interact with ANT, the voltage-dependent anion channel, and a variety of other regulatory proteins to form the PTP (14–16). Liver-specific genetic models deficient for ANT demonstrate that ANT is involved in, but is not essential for, the regulation of PT (17). Thus, an exact role for ANT remains debated, and studies are needed to further characterize the components of the PTP (18). Our studies present genetic proof that CypD is essential for PT and is the target of CsA.

A number of studies using CsA and the overexpression of CypD have implicated PT in apoptotic and necrotic cell death (12, 29–31). To investigate the role of CypD in apoptotic cell death, we challenged WT and CypD-deficient MEFs with an extensive spectrum of stimuli. WT and CypD-deficient MEFs were equally susceptible to cell death induced by the intrinsic and extrinsic pathways of apoptosis; however, CypD-deficient MEFs were significantly less susceptible to cell death induced by oxidative stress than their WT counterparts. H_2O_2 generates superoxide radicals and releases calcium from intracellular stores that is subsequently taken up by mitochondria and has been implicated in PT-dependent apoptosis (9). CypD-deficient cells were significantly protected from cell death induced by H_2O_2, implicating CypD in this paradigm of cell death. This finding is consistent with recent work by Nakagawa *et al.* (42) and Baines *et al.* (43), who have suggested a role for CypD in the regulation of necrotic cell death induced by calcium overload and oxidative stress.

In our studies, the most striking evidence signifying a role for CypD in cell death was displayed in CypD-deficient mice subjected to an MCAo model of ischemia/reperfusion injury. Infarct size in CypD-deficient mice was dramatically reduced compared with their littermate controls. These data prove that conditions required for the activation of PT are present during ischemia/reperfusion, as previously suggested (32–34, 45, 46). Neuronal cell death can occur by a diversity of mechanisms (47). Genetic models have been instrumental in defining factors contributing to cell death by ischemia/reperfusion and have implicated roles for death receptors, caspase activation, DNA damage, and oxidative stress (48). The absence of BID, a proapoptotic BCL-2 family member that is activated downstream of death receptors, reduces infarct size after mild focal

ischemia (49). In a similar model, the caspase inhibitor zVAD-fmk significantly reduces neuronal cell death (50). In our model of ischemia/reperfusion, we suggest that the absence of CypD decreases infarct size by reducing the susceptibility of cells to death. The central role of CypD in ischemia/reperfusion-induced cell death implicates it as a selective target for therapeutic interventions aimed at reducing the infarct area after an ischemic stroke.

We thank B. Malynn, S. Oakes, M. Bassik, and M. Schuler for critically reading the manuscript; E. Smith for manuscript preparation; and C. Gee. This work was supported by the Swiss National Science Foundation (A.C.S.), a Dana–Farber Cancer Institute Lee Fellowship (to A.C.S.), a Human Frontier Science Program Long Term Fellowship (to O.T.), the Cancer Research Fund of the Damon Runyon Foundation Fellowship (C.H.), the Leukemia Lymphoma Society Special Fellow Award (to N.N.D.), and National Institutes of Health Grants CA50239 (to S.J.K.), NS37141, and NS10828 (to M.A.M.).

1. Danial, N. N. & Korsmeyer, S. J. (2004) *Cell* **116,** 205–219.
2. Green, D. R. & Kroemer, G. (2004) *Science* **305,** 626–629.
3. Orrenius, S., Zhivotovsky, B. & Nicotera, P. (2003) *Nat. Rev. Mol. Cell. Biol.* **4,** 552–565.
4. Vander Heiden, M. G., Chandel, N. S., Williamson, E. K., Schumacker, P. T. & Thompson, C. B. (1997) *Cell* **91,** 627–637.
5. Scorrano, L., Ashiya, M., Buttle, K., Weiler, S., Oakes, S. A., Mannella, C. A. & Korsmeyer, S. J. (2002) *Dev. Cell* **2,** 55–67.
6. Goldstein, J. C., Waterhouse, N. J., Juin, P., Evan, G. I. & Green, D. R. (2000) *Nat. Cell Biol.* **2,** 156–162.
7. Wei, M. C., Zong, W. X., Cheng, E. H., Lindsten, T., Panoutsakopoulou, V., Ross, A. J., Roth, K. A., MacGregor, G. R., Thompson, C. B. & Korsmeyer, S. J. (2001) *Science* **292,** 727–730.
8. Bassik, M. C., Scorrano, L., Oakes, S. A., Pozzan, T. & Korsmeyer, S. J. (2004) *EMBO J.* **23,** 1207–1216.
9. Scorrano, L., Oakes, S. A., Opferman, J. T., Cheng, E. H., Sorcinelli, M. D., Pozzan, T. & Korsmeyer, S. J. (2003) *Science* **300,** 135–139.
10. Pinton, P., Ferrari, D., Magalhaes, P., Schulze-Osthoff, K., Di Virgilio, F., Pozzan, T. & Rizzuto, R. (2000) *J. Cell Biol.* **148,** 857–862.
11. Foyouzi-Youssefi, R., Arnaudeau, S., Borner, C., Kelley, W. L., Tschopp, J., Lew, D. P., Demaurex, N. & Krause, K. H. (2000) *Proc. Natl. Acad. Sci. USA* **97,** 5723–5728.
12. Bernardi, P. (1999) *Physiol. Rev.* **79,** 1127–1155.
13. Leist, M., Single, B., Castoldi, A. F., Kuhnle, S. & Nicotera, P. (1997) *J. Exp. Med.* **185,** 1481–1486.
14. Crompton, M., Virji, S. & Ward, J. M. (1998) *Eur. J. Biochem.* **258,** 729–735.
15. Halestrap, A. P., Woodfield, K. Y. & Connern, C. P. (1997) *J. Biol. Chem.* **272,** 3346–3354.
16. Woodfield, K., Ruck, A., Brdiczka, D. & Halestrap, A. P. (1998) *Biochem. J.* **336,** Part 2, 287–290.
17. Kokoszka, J. E., Waymire, K. G., Levy, S. E., Sligh, J. E., Cai, J., Jones, D. P., MacGregor, G. R. & Wallace, D. C. (2004) *Nature* **427,** 461–465.
18. Halestrap, A. P. (2004) *Nature* **430,** 1 p. following p. 983.
19. He, L. & Lemasters, J. J. (2002) *FEBS Lett.* **512,** 1–7.
20. Zoratti, M. & Szabo, I. (1995) *Biochim. Biophys. Acta* **1241,** 139–176.
21. Abdel-Hamid, K. M. & Tymianski, M. (1997) *J. Neurosci.* **17,** 3538–3553.
22. Starkov, A. A., Chinopoulos, C. & Fiskum, G. (2004) *Cell Calcium* **36,** 257–264.
23. Dirnagl, U., Iadecola, C. & Moskowitz, M. A. (1999) *Trends Neurosci.* **22,** 391–397.
24. Friberg, H. & Wieloch, T. (2002) *Biochimie* **84,** 241–250.
25. Leist, M. & Nicotera, P. (1998) *Exp. Cell Res.* **239,** 183–201.
26. Ueda, H. & Fujita, R. (2004) *Biol. Pharm. Bull.* **27,** 950–955.
27. Nicolli, A., Basso, E., Petronilli, V., Wenger, R. M. & Bernardi, P. (1996) *J. Biol. Chem.* **271,** 2185–2192.
28. Fontaine, E., Ichas, F. & Bernardi, P. (1998) *J. Biol. Chem.* **273,** 25734–25740.
29. Lin, D. T. & Lechleiter, J. D. (2002) *J. Biol. Chem.* **277,** 31134–31141.
30. Li, Y., Johnson, N., Capano, M., Edwards, M. & Crompton, M. (2004) *Biochem. J.* **383,** 101–109.
31. Schubert, A. & Grimm, S. (2004) *Cancer Res.* **64,** 85–93.
32. Khaspekov, L., Friberg, H., Halestrap, A., Viktorov, I. & Wieloch, T. (1999) *Eur. J. Neurosci.* **11,** 3194–3198.
33. Shiga, Y., Onodera, H., Matsuo, Y. & Kogure, K. (1992) *Brain Res.* **595,** 145–148.
34. Matsumoto, S., Friberg, H., Ferrand-Drake, M. & Wieloch, T. (1999) *J. Cereb. Blood Flow Metab.* **19,** 736–741.
35. Huang, Z., Huang, P. L., Panahian, N., Dalkara, T., Fishman, M. C. & Moskowitz, M. A. (1994) *Science* **265,** 1883–1885.
36. Gunter, K. K. & Gunter, T. E. (1994) *J. Bioenerg. Biomembr.* **26,** 471–485.
37. Crompton, M. (1999) *Biochem. J.* **341,** Part 2, 233–249.
38. Scaffidi, C., Schmitz, I., Zha, J., Korsmeyer, S. J., Krammer, P. H. & Peter, M. E. (1999) *J. Biol. Chem.* **274,** 22532–22538.
39. Li, H., Zhu, H., Xu, C. J. & Yuan, J. (1998) *Cell* **94,** 491–501.
40. Luo, X., Budihardjo, I., Zou, H., Slaughter, C. & Wang, X. (1998) *Cell* **94,** 481–490.
41. Basso, E., Fante, L., Fowlkes, J., Petronilli, V., Forte, M. A. & Bernardi, P. (2005) *J. Biol. Chem.*
42. Nakagawa, T., Shimizu, S., Watanabe, T., Yamaguchi, O., Otsu, K., Yamagata, H., Inohara, H., Kubo, T. & Tsujimoto, Y. (2005) *Nature* **434,** 652–658.
43. Baines, C. P., Kaiser, R. A., Purcell, N. H., Blair, N. S., Osinska, H., Hambleton, M. A., Brunskill, E. W., Sayen, M. R., Gottlieb, R. A., Dorn, G. W., *et al.* (2005) *Nature* **434,** 658–662.
44. Zamzami, N., Hirsch, T., Dallaporta, B., Petit, P. X. & Kroemer, G. (1997) *J. Bioenerg. Biomembr.* **29,** 185–193.
45. Weiss, J. N., Korge, P., Honda, H. M. & Ping, P. (2003) *Circ. Res.* **93,** 292–301.
46. Halestrap, A. P., Connern, C. P., Griffiths, E. J. & Kerr, P. M. (1997) *Mol. Cell. Biochem.* **174,** 167–172.
47. Yuan, J., Lipinski, M. & Degterev, A. (2003) *Neuron* **40,** 401–413.
48. Lo, E. H., Dalkara, T. & Moskowitz, M. A. (2003) *Nat. Rev. Neurosci.* **4,** 399–415.
49. Plesnila, N., Zinkel, S., Le, D. A., Amin-Hanjani, S., Wu, Y., Qiu, J., Chiarugi, A., Thomas, S. S., Kohane, D. S., Korsmeyer, S. J. & Moskowitz, M. A. (2001) *Proc. Natl. Acad. Sci. USA* **98,** 15318–15323.
50. Endres, M., Namura, S., Shimizu-Sasamata, M., Waeber, C., Zhang, L., Gomez-Isla, T., Hyman, B. T. & Moskowitz, M. A. (1998) *J. Cereb. Blood Flow Metab.* **18,** 238–247.